Inorganic Chemistry

ARTICLE

pubs.acs.org/IC

Naked Five-Coordinate Fe^{III}(NO) Porphyrin Complexes: Vibrational and Reactivity Features

Francesco Lanucara,[†,§] Barbara Chiavarino,[†] Maria Elisa Crestoni,[†] Debora Scuderi,[‡] Rajeev K. Sinha,[‡,∥] Philippe Maître,[*,‡] and Simonetta Fornarini[*,†]

[†]Dipartimento di Chimica e Tecnologie del Farmaco, Università di Roma "La Sapienza", P.le A. Moro 5, I-00185, Roma, Italy

[‡]Laboratoire de Chimie Physique, UMR8000 CNRS, Faculté des Sciences, Université Paris Sud, Bâtiment 350, 91405 Orsay Cedex, France

Supporting Information

ABSTRACT: Model ferric heme nitrosyl complexes, $[Fe(TPP)(NO)]^+$ and $[Fe(TPFPP)(NO)]^+$, where TPP is the dianion of 5,10,15,20-tetrakis-phenyl-porphyrin and TPFPP is the dianion of 5,10,15,20-tetrakis-pentafluorophenyl-porphyrin, have been obtained as isolated species by the gas phase reaction of NO with $[Fe^{III}(TPP)]^+$ and $[Fe^{III}(TPFPP)]^+$ ions delivered in the gas phase by electrospray ionization, respectively. The so-formed nitrosyl complexes have been characterized by vibrational spectroscopy also exploiting ^{15}N-isotope substitution in the NO ligand. The characteristic NO stretching frequency is observed at 1825 and 1859 cm^{-1} for $[Fe^{III}(TPP)(NO)]^+$ and $[Fe^{III}(TPFPP)(NO)]^+$ ions, respectively, providing reference values for genuine five-coordinate Fe^{III}(NO) porphyrin complexes differing only for the presence of either phenyl or pentafluorophenyl substituents on the meso positions of the porphyrin ligand. The vibrational assignment is aided by hybrid density functional theory (DFT) calculations of geometry and electronic structure and frequency analysis which clearly support a singlet spin electronic state for both $[Fe(TPP)(NO)]^+$ and $[Fe(TPFPP)(NO)]^+$ complexes. Both TD-DFT and CASSCF calculations suggest that the singlet ground state is best described as $Fe^{II}(NO^+)$ and that the open-shell AFC bonding scheme contribute for a high-energy excited state. The kinetics of the NO addition reaction in the gas phase are faster for $[Fe^{III}(TPFPP)]^+$ ions by a relatively small factor, though highly reliable because of a direct comparative evaluation. The study was aimed at gaining vibrational and reactivity data on five-coordinate Fe^{III}(NO) porphyrin complexes, typically transient species in solution, ultimately to provide insights into the nature of the Fe(NO) interaction in heme proteins.

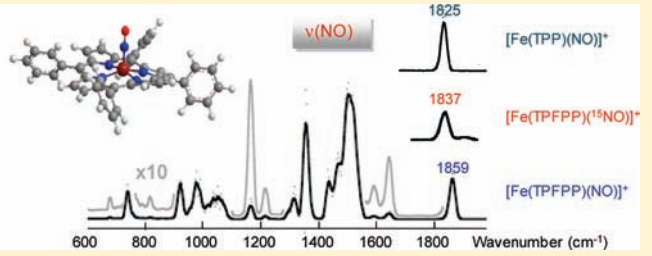

INTRODUCTION

Nitric oxide is a toxic compound that is involved, however, in a variety of important biological processes.[1] The coordination of NO to the metal center of heme enzymes is an essential part of the activation of this small molecule, at the basis of such diverse functions as nerve-signal transduction, vasodilation, blood clotting and immune response.[2]

The functions of heme cofactors are tuned by the protein environment encompassing a wide range of bonding and nonbonding interactions that affect the heme and its axial ligands. To gain an understanding of the basic elements affecting the NO interaction with hemes, synthetic metalloporphyrins have been examined and their reactivity and structure have been elucidated.[3] We now focus our interest on Fe^{III}(NO) porphyrin complexes. The $\{Fe(NO)\}^6$ electronic structure characterizes Fe^{III}(NO) porphyrin complexes according to the Enemark−Feltham notation, where the exponent 6 refers to the number of Fe d electrons plus the unpaired electron of NO.[4] The singlet ground state of these complexes can be described by the $Fe^{II}(NO^+)$ resonance structure ; with two favorable 2-electron/2-orbitals interaction between the filled d_π orbitals on the metal and the empty π^* orbitals of the nitrosyl ligand. A linear $\{Fe(NO)\}^6$ unit is thus expected, at variance with the bent FeNO geometries of $\{Fe(NO)\}^7$ compounds because of an unfavorable 3-electron/2-orbitals interaction. It has been pointed out that the vibrational modes involving the FeNO unit are sensitive to the protein environment such as distal electrostatic fields as well as to the electronic properties of peripheral substituents on the porphyrin macrocycle.[5] Both factors should modulate the electron distribution on high-energy occupied molecular orbitals (MOs) in the FeNO region. Accordingly, the N−O stretching frequency has appeared to be a good probe for nearby electrostatic perturbations because of mutations in the distal pocket.[6] However, detailed vibrational studies of ferric heme NO model complexes present complex facets.[7] Among the several factors to be taken into account one has to consider the important effects exerted by trans axial ligands. For example, the $\{Fe(NO)\}^6$ triatomic unit is bent in six-coordinate heme proteins and model complexes in the presence of thiolate ligands or of strongly σ bonding aryl groups trans to NO.[3c,8] S-donor ligands are indicated to exert a σ-trans effect on the bound NO contributing to Fe−N−O bending.[8d] Changes in the length of the Fe

Received: January 12, 2011
Published: April 08, 2011

bond to the trans axial ligand is also found to affect the N−O stretching frequency, ν(N−O).[9] Striving for a simple model containing {Fe(NO)}^{6} in a genuine five coordinate porphyrin complex, we turned to gas phase studies, operating in a medium where environmental effects are negligible and the intrinsic structural and reactivity features of the species of interest may be identified. Working in the gas phase we are in a position to inquire about intramolecular factors affecting the vibrational properties of the {Fe(NO)}^{6} unit, as distinct from environmental factors such as crystal packing effects, the presence of solvent molecules, or the proximity of counterions.

To ascertain the sensitivity of heme nitrosyl complexes to the coordination environment, two model complexes $[Fe(P)(NO)]^+$ are considered where the porphyrin ligand P is either the 5,10,15,20-meso-tetrakis(phenyl)porphinato or the 5,10,15,20-meso-tetrakis(pentafluorophenyl)porphinato dianions (TPP and TPFPP, respectively). In these complexes, differing by the presence of either C_6H_5 or C_6F_5 substituents on the four meso positions, the net electronic effect of the two different groups should be appreciable in view of the distinct electron withdrawing properties of the fluorinated phenyl ring. According to density functional theory (DFT) calculations it is found that along with progressive addition of electron density at the meso positions by π-donors such as NH_2, ν(N−O) decreases while the N−O bond length increases, and bending of the FeNO moiety becomes increasingly pronounced.[5a] Because the binding of NO to heme sites of enzymes is crucial for the activity of this diatomic molecule it is expected that NO, a "noninnocent" ligand, significantly changes the electronic structure upon binding, thus affecting the corresponding vibrational features.

The present report aims to provide benchmarks for higher order (bio)chemical perturbations, such as those brought about by trans axial ligands and by functional groups introduced as mimics of the protein environment. Useful insight may thus be gained into the NO-binding process. Vibrational spectroscopy based on IR and resonance Raman studies has afforded valuable information into the FeNO interaction in heme proteins and model porphyrin complexes in condensed phases.[5−10] In the present gas phase study IR multiple photon dissociation spectroscopy (IRMPD)[11] is exploited to probe the NO vibration in $[Fe(TPP)(NO]^+$ and $[Fe(TPFPP)(NO)]^+$ nitrosyl complexes. IRMPD spectra have been recorded using the instrumental platform at CLIO (Centre laser infrarouge d'Orsay) where an FT-ICR mass spectrometer is coupled to the IR beamline of a free electron laser (FEL). Based on this configuration, IRMPD spectroscopy has allowed to unveil the vibrational and structural features of a variety of ionic species.[12] The results of IRMPD spectroscopy are complemented by DFT and CASSCF calculations of the electronic, structural, and vibrational features of the sampled nitrosyl complexes and by kinetic measurements of the NO ligand addition reaction.

RESULTS AND DISCUSSION

The nitrosyl complexes are obtained by the gas phase nitrosylation of $[Fe^{III}(TPP)]^+$ and $[Fe^{III}(TPFPP)]^+$. The gas phase reaction of NO with $[Fe^{III}(TPFPP)]^+$ and with other $[Fe^{III}(P)]^+$ species, including iron(II) and iron(III) hemes, has already been described.[13,14] The addition of NO to naked iron porphyrin complexes is the net event at the basis of the heme-nitric oxide interaction, and the gas phase synthesis offers an efficient route to obtain Fe^{III}(NO) porphyrin complexes whose preparation in condensed phases faces problems because of their limited stability against parasitic reactions, such as loss of the ligand and reductive nitrosylation processes leading to the reduced iron species.[15] The reaction is also complicated by the presence of other nitrogen oxides when operating in the necessary excess NO. Moreover {Fe(NO)}^{6} complexes in solution are known to bind a sixth ligand or solvent molecule at the axial position trans to NO.

IRMPD Spectroscopy. The genuine five-coordinate Fe^{III}-(NO) porphyrin complexes formed in the gas phase are transferred in the cell of the FT-ICR mass spectrometer where they are irradiated by the IR beam of the FEL tuned in the 600−2000 cm^{-1} energy range. A fragmentation process is triggered by the absorption of multiple photons when the laser frequency is tuned on resonance with an active vibrational mode. The observed fragmentation process proceeds exclusively by loss of NO (eq 1). An approximate estimate for the thermodynamic threshold of the dissociation process can be obtained from the binding energies of NO to Fe^{III}-heme ions in the gas phase, varying between 104 and 124 kJ mol^{-1} as determined by experimental methods based on radiative association kinetics or equilibrium measurements.[14]

$$[Fe(P)(NO)]^+ + nh\nu \rightarrow [Fe^{III}(P)]^+ + NO \qquad (1)$$

This energy threshold requires the absorption of more than six photons at a representative wavenumber of 1500 cm^{-1}. The sequential, fast absorption of multiple photons is ensured by the high fluence of the FEL beam. Indeed, in correspondence of highly active modes, the fragmentation of the parent ion goes almost to completion and the use of attenuators and/or reduced irradiation times is warranted. The IRMPD spectrum of $[Fe(TPP)(NO)]^+$ reported in Figure 1a is obtained plotting the photodissociation yield R ($R = -\ln[I_{[Fe(P)(NO)]^+}/(I_{[Fe(P)(NO)]^+} + I_{[Fe(P)]^+})]$ where I is the ion abundance of either the parent $[Fe(P)(NO)]^+$ or the fragment $[Fe^{III}(P)]^+$ ion) as a function of the photon wavenumber. The spectrum is characterized by two intense bands at 1355 and 1825 cm^{-1}. Other distinct bands may be observed at 725, 986, 1293, and 1448 cm^{-1}. Bandwidths in IRMPD spectra are affected by several factors including the line width of the FEL (ca. 0.5% of the central wavelength), the rotational contour, and the multiphoton character of the IRMPD process.[11a,16] The observed bandwidth (full width at half-maximum, fwhm) of sharp features is 15 cm^{-1}. This bandwidth is typically observed when ions are thermalized through multiple collisions with rare gas atoms.[12a] The IR feature of major interest in this study, namely, the NO stretching mode, is responsible for the band at 1825 cm^{-1} in an otherwise blank portion of the spectrum. However, to confirm the assignment, the same IRMPD spectrum has been recorded on a ^{15}N-labeled complex obtained by the reaction of $[Fe^{III}(TPP)]^+$ with ^{15}NO. As shown in Figure S1 (in the Supporting Information) the feature at 1825 cm^{-1} is clearly isotope sensitive, shifting to 1792 cm^{-1} in the spectrum of the ^{15}N-labeled compound. A red shift of this size is consistent with the stretching vibration of an NO oscillator.[16,17]

The NO stretching mode is rather found at 1859 cm^{-1} in the IRMPD spectrum of $[Fe(TPFPP)(NO)]^+$ shown in Figure 1b, characterized by two other major bands at 1355 and 1501−1514 cm^{-1}. Other significant bands appear at 742, 920, 984, 1044−1071, 1160, 1314, 1436, 1469, and 1642 cm^{-1}. Also for this complex the consequence of ^{15}N-labeling of the nitric oxide ligand on the experimental IRMPD spectrum has been inspected. The spectrum of $[Fe(TPFPP)(^{15}NO)]^+$ displayed in Figure S2 (in the Supporting Information) shows a sizable

dx.doi.org/10.1021/ic200073v |Inorg. Chem. 2011, 50, 4445–4452

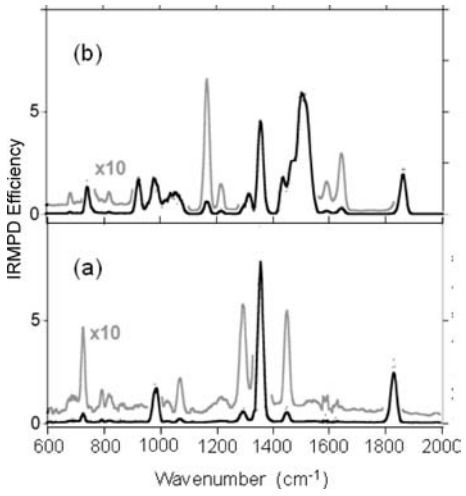

Figure 1. IRMPD spectra of $[Fe(TPP)(NO)]^+$ (a) and of $[Fe(TPFPP)(NO)]^+$ (b).

change in the position of the band ascribed to NO stretching, now shifted to 1837 cm^{-1}. Once again the observed red shift is compatible with an NO stretching vibration.

The low-frequency region is expected to reveal vibrational modes involving Fe−NO stretching and bending of the FeNO unit. To this end the 450−850 cm^{-1} wavenumber region has been carefully explored. The so-investigated portion of the IRMPD spectrum of $[Fe(TPFPP)(NO)]^+$ is plotted in Figure S3 (in the Supporting Information). It confirms the presence of the prominent band at 742 cm^{-1} and of the weaker feature at 689 cm^{-1} (profile (a) in Figure S3). Another absorption, however faint, appears at 707 cm^{-1} while no further activity is observed down to 450 cm^{-1}. The IRMPD spectrum of $[Fe(TPFPP)(^{15}NO)]^+$ recorded in the 620−710 cm^{-1} range shows that the two features recorded for the unlabeled complex at 689 and 707 cm^{-1} are now observed at 676 and 697 cm^{-1}, respectively (profile (b) in Figure S3). A similar, extended scrutiny was not performed on the spectrum of $[Fe(TPP)(NO)]^+$ in consideration of the congested IRMPD activity in the 660−710 cm^{-1} range of interest.

It is interesting to notice that the frequency of the NO stretching vibration for the $[Fe(TPP)(NO)]^+$ complex (at 1825 cm^{-1}) and for $[Fe(TPFPP)(NO)]^+$ (at 1859 cm^{-1}) fall close to the range of the NO stretching mode of $[Fe(OEP)(NO)]ClO_4$ (where OEP is the dianion of octaethylporphyrin) recorded at 1838 and 1868 cm^{-1} for two different crystalline forms.[5e] Crystal packing effects and the presence of the counterion may, however, affect the NO stretching vibration of this five-coordinate complex, possibly ending in a fortuitous cancellation of effects.

In the sampled $[Fe(TPP)(NO)]^+$ and $[Fe(TPFPP)(NO)]^+$ complexes, the electronic properties are modulated by the modification of the porphyrin periphery, and the effect is significant with a blue shift of more than 30 cm^{-1} when the phenyl substituents are replaced with pentafluorophenyl groups. The sensitivity of the FeNO bonding to intramolecular (peripheral and proximal) modification as well as intermolecular distal perturbations has been studied by DFT calculations both in five- and six-coordinate $\{Fe(NO)\}^6$ porphyrin complexes.[5] Several types of influences are found to affect the FeNO bonding parameters whereby a dominant role is played by the electron density perturbation in high energy molecular orbitals.[5,18] We now focus on the differential effect of C_6H_5 versus C_6F_5 substitutents on the four porphyrin meso positions observing that the

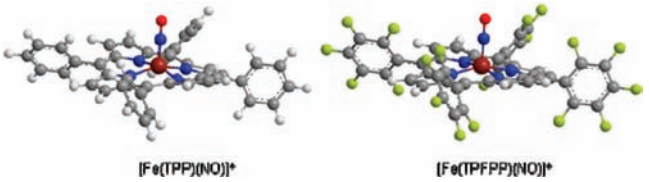

Figure 2. Optimized (C_{2v}) structures of $[Fe(TPP)(NO)]^+$ and $[Fe(TPFPP)(NO)]^+$ complexes.

strong electron withdrawing effect of the C_6F_5 groups causes a blue shift of the NO stretching frequency, as shown by the experimental finding of the NO stretching at 1859 cm^{-1} in the IRMPD spectrum of $[Fe(TPFPP)(NO)]^+$, as compared with 1825 cm^{-1} for $[Fe(TPP)(NO)]^+$.

The correlation of ν(Fe−NO) and ν(N−O) values in Fe^{III}-(NO) porphyrin complexes is the topic of high current interest.[5,7] The two frequencies are directly correlated in six-coordinate $\{Fe(NO)\}^6$ complexes with an axial thiolate ligand. Both values appear to decrease (increase) in concert. For imidazole ligated $Fe^{III}(NO)$ porphyrinates in myoglobin variants ν(Fe−NO) and ν(N−O) are negatively correlated.[5d] The negative correlation is consistent with backbonding, exerting a major role in the $Fe^{II}(NO^+)$ representation of the ground state of $\{Fe(NO)\}^6$ complexes.[7] Where backbonding is more pronounced, the Fe−NO bond is strengthened while the N−O bond is weakened because of increased electron density in the π^* orbitals. In addition to this gross effect, and possibly overriding it, a number of additional subtle factors need to be taken into account, as described in detail in a recent report.[5d] Thiolate ligation presents a positive ν(Fe−NO)/ν(N−O) correlation arising from Fe^{III}−N−O bending. In this context, it would be desirable to ascertain the behavior of ν(Fe−NO)/ν(N−O) within models such as the gaseous $[Fe(TPP)(NO)]^+$ and $[Fe(TPFPP)(NO)]^+$ five-coordinate complexes.

One further consideration regards the possible occurrence of linkage isomers of the $Fe^{III}(NO)$ porphyrin complexes, where the coordination mode for the nitrosyl ligand may be either η^1-O or η^2-NO. Both isomers Fe(η^1-ON) and Fe(η^2-ON) are calculated to lie higher in energy by more than one eV with respect to the nitrosyl Fe(η^1-NO) complex.[19] The isonitrosyl Fe(η^1-ON) complex may be obtained from the nitrosyl by photolysis of $\{Fe(NO)\}^6$ porphyrin complexes at low temperature and is characterized by a significantly lower ν(O−N) (by ca. 180 cm^{-1} with respect to ν(N−O)).[20] It may thus be concluded that the observed values of ν(N−O) rather rule out the presence of this linkage isomer.

Computed Geometries and Electronic States. As it is usually performed when IRMPD spectroscopy is used to gain geometric and electronic structure elucidation, calculations have been carried out on the potential candidates for the species being assayed. The structure of the $[Fe(TPP)(NO)]^+$ and $[Fe(TPFPP)(NO)]^+$ complexes in their singlet spin state have been optimized using a C_{2v} symmetry restriction. The C_{2v} optimized geometries of these complexes in the ground $^1A_1$ electronic state are illustrated in Figure 2, and a few geometrical parameters are listed in Table 1. In particular, one may note that the Fe−NO bond distance is quite short, comparable to the Fe−NO bond length of 1.64 Å observed in the crystal structure of five-coordinate $[Fe(OEP)(NO)]ClO_4$.[3d]

A large number of studies have addressed the metal-NO interaction in iron(II) and iron(III) nitrosyl complexes with porphyrin ligands.[19,21] The electronic structure associated with the $\{Fe(NO)\}^6$ subunit, the core of the complex presently investigated,

dx.doi.org/10.1021/ic200073v |Inorg. Chem. 2011, 50, 4445–4452

Table 1. Selected, Calculated Geometrical Parameters of $[Fe(TPP)NO]^+$ and $[Fe(TPFPP)NO]^+$ Complexes[a]

	$[Fe(TPP)NO]^+$	$[Fe(TPFPP)NO]^+$
Fe−NO bond length	1.597	1.598
N−O bond length	1.150	1.145
$C_{meso}-C_{phenyl}$	1.492	1.491
FeNO angle	180	180

[a] Bond lengths in Å, bond angles in degrees.

Scheme 1. Electronic Structures Illustrating the Distinct Ways of the Electron Distribution for Singlet $\{Fe(NO)\}^6$ Complexes: Closed Shell $[Fe^{II}NO^+]$ (a); Open Shell Antiferromagnetic Coupling (AFC) of Doublet Spin State Fe^{III} Coupled with an NO Radical $[Fe^{III}NO]$ ((b) and (c))

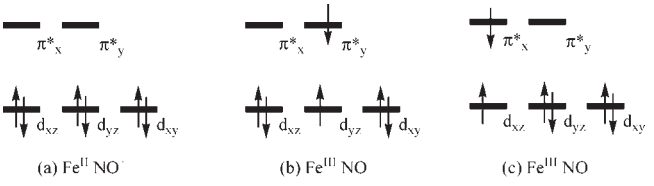

may be envisioned as an Fe^{III} coupled with an NO radical $[Fe^{III}NO]$ or as an Fe^{II} interacting with an NO^+ cation $[Fe^{II}NO^+]$. Assuming a strong ligand field about the $\{Fe(NO)\}^6$ unit, a singlet electronic ground state should be expected. This ground state may thus correspond to a closed shell electronic $[Fe^{II}NO^+]$ configuration (Scheme 1a), or to a so-called antiferromagnetic coupling (AFC) of Fe^{III} and NO $[Fe^{III}NO]$ as depicted in Scheme 1b−c. In a recent detailed study[7] of the electronic structure of a six-coordinate $\{Fe(NO)\}^6$ complex, these two bonding schemes were envisaged and two types of calculation were performed. A restricted B3LYP calculation was performed, thus associated with an $[Fe^{II}NO^+]$ configuration (Scheme 1a), leading to a structure characterized by a short Fe−NO distance (~1.64 Å). A longer Fe−NO bond length (1.69 Å) was reported for a structure optimized using an unrestricted B3LYP approach, and the reported spin density on the Fe and N atoms (+0.84 and −0.73) suggests that this structure corresponds to an AFC type electronic state such as depicted in Scheme 1b−c. Using the unrestricted approach, the B3LYP energy was found to be within 4 kJ/mol of the one found using the restricted approach. It was concluded that two singlet spin states with two different electronic configurations lie within few kJ/mol.[7]

To gain insights into the relative energy of the two $[Fe^{III}NO]$ and $[Fe^{II}NO^+]$ bonding schemes depicted in Scheme 1, two quantum chemical methods were used. The $[Fe(TPP)(NO)]^+$ complex was considered in its C_{2v} geometry corresponding to the $^1A_1$ state optimized using the restricted B3LYP approach. Using this geometry, two approaches were used for evaluating the relative energy of the $[Fe^{III}NO]$ and $[Fe^{II}NO^+]$ electronic configurations.

CASSCF calculations have been performed, first on the five-coordinate $[Fe(TPP)(NO)]^+$ complex, but also on the six-coordinate complex resulting from the addition of an imidazole ligand, already discussed by Lehnert et al.[7] The active space was chosen so as to consider the electronic configurations associated with the distribution of six electrons in the three nonbonding d orbitals and two NO π^* orbitals (see Scheme 1). As a result, the

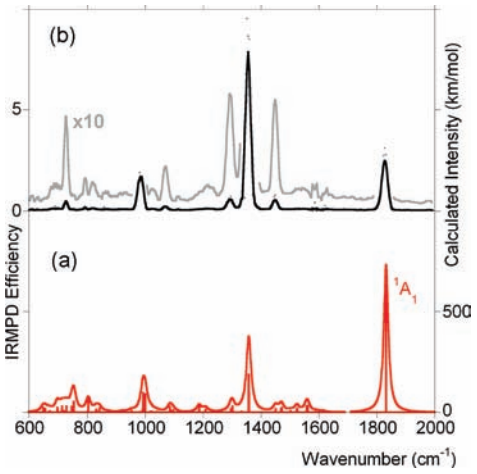

Figure 3. Calculated IR spectrum of the $[Fe(TPP)(NO)]^+$ complex (a) and experimental IRMPD spectrum (b).

CASSCF wave function was the outcome of the variational optimization of the $[Fe^{II}NO^+]$ closed-shell electronic configuration with the ones corresponding to the AFC of Fe^{III} and an NO radical. Using the RB3LYP optimized C_{2v} geometry of the $^1A_1$ state, the predicted ground state at the CASSCF level essentially corresponds to an $[Fe^{II}NO^+]$ closed-shell electronic configuration (coefficient = 0.92). The electronic configuration associated with AFC of Fe^{III} and NO yields only a small contribution to the ground electronic state at the equilibrium geometry (0.07).

The electronic excited states were then obtained through a configuration interaction calculation using the CASSCF orbitals. The electronic excited $^1A_1$ state mainly corresponding to the AFC electronic configurations was found to be 420 kJ mol^{-1} above the electronic ground state. The electronic excitation is probably overestimated because the orbitals were optimized for the ground $^1A_1$ closed-shell electronic state. A similar calculation scheme was applied to characterize the electronic states of $[Fe(TPP)(imidazole)(NO)]^+$ complex. At the RB3LYP optimized geometry, the analysis of the CASSCF ground state wave function clearly shows that the dominant electronic configuration corresponds to an $[Fe^{II}NO^+]$ closed-shell electronic configuration (coefficient = 0.91). As for the above-discussed $[Fe(TPP)(NO)]^+$ complex, the contribution of the AFC electronic configurations to the singlet ground state is marginal (coefficient = 0.09). The excited electronic state associated with the AFC of Fe^{III} and NO was found to be significantly higher in energy (346 kJ mol^{-1}). Alternatively, the energy gap was also evaluated using the TD-DFT approach and the B3LYP hybrid density functional. At this level of theory, the excitation energy value was estimated to be 191 kJ mol^{-1}.

It thus seems clear that the bonding scheme in the $[Fe(TPP)(NO)]^+$ complex corresponds to the interaction of a closed-shell Fe^{II} with an NO^+ cation. The analysis of the RB3LYP vibrational frequencies ensures the identification of the computed C_{2v} species as a minimum and provides the basis for the calculation of the IR spectra to be compared with the experimental IRMPD spectra in the following paragraph.

Calculated IR Spectra and Experimental IRMPD Spectra. The IR spectrum calculated for the ground $^1A_1$ electronic state of the $[Fe(TPP)(NO)]^+$ complex is reported in Figure 3a to be compared with the experimental IRMPD spectrum displayed in

dx.doi.org/10.1021/ic200073v |Inorg. Chem. 2011, 50, 4445–4452

Table 2. Experimental IRMPD Bands Observed for $[Fe(TPP)NO]^+$ and Suggested Assignment to IR Transitions

experimental IRMPD[a]	calculated IR[b]	vibrational mode
	650 (23)	porphyrin and phenyl def
680 (0.020)	695 (30)	porphyrin ring def
702 (0.022)	696 (24)	phenyl CH bend
725 (0.098)	729 (31)	CH bend, Fe−NO stretch
	754 (53)	porphyrin ring def
790 (0.021)	803 (66)	pyrrolic CH bend
819 (0.047)	831 (14)	porphyrin ring def
986 (0.359)	994 (97)	porphyrin ring def
	1000 (90)	porphyrin ring def
	1025 (0.022)	porphyrin ring def
1069 (0.044)	1085 (13)	phenyl and pyrrolic CH bend
	1097 (11)	phenyl and pyrrolic CH bend
1114 (0.013)	1187 (17)	CH bend, phenyl group bend
1220 (0.026)	1209 (13)	porphyrin def
1293 (0.119)	1296 (18)	porphyrin def
	1302 (31)	porphyrin def
1355 (1.000)	1357 (188)	porphyrin def
	1359 (188)	porphyrin def
1448 (0.074)	1471 (24)	porphyrin def
	1470 (18)	porphyrin def
1518 (0.015)	1525 (20)	porphyrin def
	1524 (13)	porphyrin def
1558 (0.013)	1561 (33)	porphyrin def
1825 (0.312)	1832 (734)	NO stretch

[a] Band positions (cm^{-1}) and relative intensities (in parentheses). [b] IR transitions (cm^{-1}) and intensities (km mol^{-1},in parentheses).

the b panel of the same figure. The calculated harmonic frequencies are scaled by a factor of 0.975 except the NO stretching mode. This mode is known to require a smaller scaling factor[5d,22] and the value of 0.92 determined by Pulay and coworkers from the analysis of DFT calculated frequencies of nitroso compounds[23] is conveniently adopted.

As shown in Figure 3 the appropriately scaled IR spectrum shows a remarkable agreement with the IRMPD spectrum of $[Fe(TPP)(NO)]^+$, supporting the assignment of an $^1A_1$ electronic state. The calculated IR spectrum properly accounts for the observed IRMPD features both regarding their frequency and, more approximately, their relative intensity also in the 1000−1600 cm^{-1}, so-called fingerprint, region. The major vibrational modes are summarized in Table 2 together with the experimental IRMPD bands. Also the analysis of the tabulated data confirms the qualitative agreement appearing in Figure 3. In particular one may note that the IRMPD band at 1825 cm^{-1} is accounted for by the NO stretching mode calculated at 1832 cm^{-1}. The effect of ^{15}N-labeling of the nitric oxide ligand yields an expected red shift in the calculated IR spectrum of $[Fe(TPP)(^{15}NO)]^+$, displaying the $^{15}N-O$ stretching frequency at 1798 cm^{-1}, only 6 cm^{-1} apart from the experimental band at 1792 cm^{-1} (Figure S4 in the Supporting Information).

As already ascertained for the $[Fe(TPP)(NO)]^+$ complex, also the $[Fe(TPFPP)(NO)]^+$ complex presents an IRMPD spectrum matching the calculated IR spectrum of the $^1A_1$ electronic state. The qualitative agreement of the two profiles is apparent in Figure 4(a,b) while a detailed account of the major

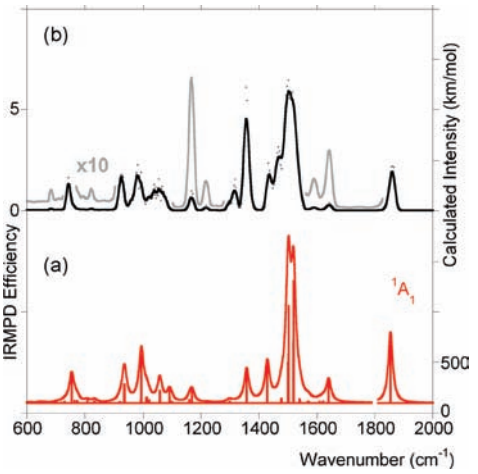

Figure 4. Calculated IR spectrum of the $[Fe(TPFPP)(NO)]^+$ complex (a) and experimental IRMPD spectrum (b).

vibrational features is given in Table 3. The notably high activity of the porphyrin and phenyl breathing modes is due to the presence of the fluoro substituents, likely responsible for pronounced dipole moment changes upon vibrational transitions.

The NO stretching mode, the landmark IRMPD feature at 1859 cm^{-1}, is calculated at 1855 cm^{-1}. The observed red shift at 1837 cm^{-1} for the ^{15}N-labeled complex, $[Fe(TPFPP)(^{15}NO)]^+$, is again fairly consistent with the value of 1814 cm^{-1} obtained by calculations. Figure S5 in the Supporting Information allows the direct comparison of the IRMPD spectrum and the calculated IR spectrum for the $[Fe(TPFPP)(^{15}NO)]^+$ complex.

In the low frequency region, a careful analysis of the normal modes suggests that three of them involve Fe−NO stretching coupled with porphyrin ring local modes, and the calculated frequencies are 702, 720, and 731 cm^{-1} (Table 3). The total predicted red-shift upon substituting ^{15}NO for ^{14}NO is 5 cm^{-1}. On the other hand, the normal modes involving the Fe−N−O bending modes are predicted at lower frequencies (~430 cm^{-1}) with very low intensity (1 km mol^{-1}). On this basis one may conclude that the observed band at 689 cm^{-1} and the weaker feature at 707 cm^{-1} are associated with the Fe−NO stretching mode of $[Fe(TPFPP)(NO)]^+$.

Kinetic Study of NO Binding. A kinetic study of NO binding to form $[Fe(TPP)(NO)]^+$ and $[Fe(TPFPP)(NO)]^+$ complexes has been carried out to further characterize the NO interaction with heme models. The reaction rates for NO binding to $[Fe(TPP)]^+$ and $[Fe(TPFPP)]^+$ (eq 2, where P is TPP or TPFPP) were thus examined using FT-ICR mass spectrometry.

$$[Fe(P)]^+ + NO \rightarrow [Fe(P)(NO)]^+ \qquad (2)$$

The evaluation of the absolute rate constants is known to suffer mainly from the uncertainty about the pressure of the neutral in the FT-ICR cell (NO in the present case)[14b] and an error of ±30% is estimated to affect the second order rate constants and the derived reaction efficiencies (Φ). To circumvent this problem, the NO addition reaction was allowed to occur admitting both $[Fe(TPP)]^+$ and $[Fe(TPFPP)]^+$ ions into the cell and recording the time dependence of the abundance of reagent and adduct ions in the same run. Kinetic runs were performed at different values of NO pressure, maintained constant during each run. The so-obtained kinetic

dx.doi.org/10.1021/ic200073v |Inorg. Chem. 2011, 50, 4445–4452

Table 3. Experimental IRMPD Bands Observed for $[Fe(TPFPP)NO]^+$ and Suggested Assignment to IR Transitions

experimental IRMPD[a]	calculated IR[b]	vibrational mode
689 (0.026)	702 (8)	Fe−NO stretch, porphyrin ring def
707 (0.009)	720 (5)	Fe−NO stretch, porphyrin ring def
	731 (15)	Fe−NO stretch, porphyrin ring def
742 (0.264)	755 (144)	porphyrin ring def
767 (0.058)	764 (25)	pyrrolic CH bend, phenyl def
793 (0.022)	774 (21)	pyrrolic CH bend, phenyl def
	775 (20)	pyrrolic CH bend, phenyl def
820 (0.034)	807 (24)	pyrrolic CH bend
920 (0.300)	934 (180)	porphyrin ring def
	936 (180)	porphyrin ring def
984 (0.448)	995 (469)	C−F stretch
	1010 (50)	porphyrin ring def
	1013 (53)	porphyrin ring def
	1021 (28)	porphyrin ring def
∼1044 (0.285)	1056 (117)	pyrrolic CH bend, phenyl def
∼1071 (0.240)	1059 (117)	pyrrolic CH bend, phenyl def
	1092 (62)	pyrrolic CH bend
1160 (0.118)	1168 (64)	porphyrin and phenyl group def
	1168 (61)	porphyrin and phenyl group def
1209 (0.077)	1217 (10)	porphyrin and phenyl group def
1314 (0.169)	1298 (11)	porphyrin and phenyl group def
	1300 (15)	porphyrin and phenyl group def
1355 (0.767)	1357 (158)	pyrrolic CH bend
	1358 (164)	pyrrolic CH bend
1436 (0.306)	1429 (193)	porphyrin and phenyl group def
1469 (0.449)	1476 (43)	pyrrolic CH bend. porphyrin def
	1477 (43)	pyrrolic CH bend. porphyrin def
1501 (1.000)	1500 (225)	phenyl group def
	1501 (959)	phenyl group def
1514 (0.924)	1519 (620)	porphyrin and phenyl group def
	1519 (620)	porphyrin and phenyl group def
1589 (0.027)	1569 (11)	porphyrin def
	1572 (13)	porphyrin def
1642 (0.050)	1641 (111)	C−C (phenyl group) stretch
1859 (0.325)	1855 (696)	NO stretch

[a] Band positions (cm^{-1}) and relative intensities (in parentheses). [b] IR transitions (cm^{-1}) and intensities (km mol^{-1}, in parentheses).

Table 4. Kinetic Data for the Addition Reaction of NO with $[Fe(P)]^+$ Complexes (P = TPP, TPFPP)

$[Fe(P)]^+$	k_{exp}[a]	Φ[b]
$[Fe(TPP)]^+$	0.35	4.9
$[Fe(TPFPP)]^+$	0.55	7.8

[a] Second order rate constant for the reaction $[Fe(P)]^+ + NO \rightarrow [Fe(P)(NO)]^+$, in units of 10^{-10} cm^3 $molecule^{-1}$ s^{-1}, at the temperature of the FT-ICR cell of 300 K. [b] $\Phi = k_{exp}/k_{coll} \times 100$.

data are reported in Table 4. Because of the adopted procedure, the relative rates are highly reliable and the ratio of 1.6 clearly indicates that $[Fe(TPFPP)]^+$ binding is faster.

CONCLUSIONS

Several detailed vibrational studies of ferric heme model complexes have been reported,[5,10,21] none of them, however, dealing with naked five-coordinate $\{Fe(NO)\}^6$ complexes. The gaseous environment, where the $Fe^{III}(NO)$ porphyrin complexes have been formed and assayed as described in this study, has provided a suitable medium to obtain genuine five coordinate ferric nitrosyl complexes, endowed with a lifetime long enough to undergo IRMPD spectroscopy. By these means, the selected $[Fe(TPP)(NO)]^+$ and $[Fe(TPFPP)(NO)]^+$ complexes are found to display $\nu(N-O)$ frequency values of 1825 and 1859 cm^{-1}, respectively. These values encompass the $\nu(N-O)$ frequency of 1842 cm^{-1} previously reported for the prototypical heme nitrosyl complex $[Fe(PP\text{-}IX)(NO)]^+$ (where PP-IX is the dianion of protoporphyrin IX).[16]

A $[Fe^{II}NO^+]$ core for the ground state electronic structure of these $\{Fe(NO)\}^6$ species is consistent with the observed frequency values falling within the range typical for ferric heme NO adducts in proteins and model complexes, while $\{Fe(NO)\}^7$ complexes holding a $[Fe^{II}NO]$ core display typical NO stretching frequencies in the range of 1600−1700 cm^{-1}.[5,10,21] However, the conclusive assignment of the electronic structure has been allowed by the DFT calculation of the optimized geometries and the IR spectra of the complexes in the singlet $^1A_1$ electronic state. The calculated IR spectra account for the observed IR features of both $[Fe^{III}(TPP)NO]^+$ and $[Fe^{III}(TPFPP)NO]^+$ complexes. The assignment of the singlet state to these gaseous five coordinate ferric nitrosyl complexes finds a counterpart in the diamagnetic properties of $\{Fe(NO)\}^6$ complexes in protein and condensed phase environments. At the same time it provides further evidence on the proper use of B3LYP calculated IR spectra to aid in the assignment of the observed experimental IRMPD features and on the recognized performance of hybrid DFT methods in fulfilling this task.[24] DFT calculations have allowed a complete analysis of the vibrational spectra of $Fe^{III}(TPP)Cl$[25] while they have been found problematic in reproducing the vibrational energies and normal mode descriptions of the Fe−N−O unit in five coordinate ferrous heme nitrosyls.[19e]

An interesting facet of the comparative spectroscopic and reactivity behavior of $[Fe^{III}(TPP)NO]^+$ and $[Fe^{III}(TPFPP)NO]^+$ complexes is the quite similar structure, yet markedly different electronic effect of the four meso substituents, allowing a meaningful comparison of the changes brought about by the phenyl versus pentafluorophenyl substitution.

A complementary piece of information regards the relative reactivity of $[Fe^{III}(TPP)]^+$ and $[Fe^{III}(TPFPP)]^+$ in the NO addition reaction. Further spectroscopic data on five coordinate ferric nitrosyl complexes in the gas phase are clearly desirable to deepen our understanding of the intrinsic features of NO binding to ferric hemes.

EXPERIMENTAL SECTION

IRMPD Experiments. The ionic precursors of the nitrosyl complexes, $[Fe^{III}(TPP)]^+$ and $[Fe^{III}(TPFPP)]^+$, were obtained by electrospray ionization (ESI) of a methanol solution of the respective chlorides ($Fe^{III}(TPP)Cl$ and $Fe^{III}(TPFPP)Cl$, commercial products from Sigma Aldrich). The ESI-formed ions were mass selected and allowed to react with NO seeded in the argon flowing in the hexapole accumulation trap of the 7T hybrid FT-ICR mass spectrometer (Bruker Apex Qe). The nitrosyl complexes $[Fe(TPP)NO]^+$ and $[Fe(TPFPP)NO]^+$ were thus allowed to thermalize and in particular to release any excess energy

gained in the addition reaction by unreactive collisions with argon. They were pulse-driven into the FT-ICR cell, mass selected, and irradiated by the tunable IR-FEL light. The design of the experimental set up has been already described in detail.[12a] When the photon energy is resonant with an active vibrational mode of the sampled ion, a fragmentation process may ensue, activated by the energy gained by a sequence of resonant photon absorption events combined with intramolecular vibrational energy redistribution.[11] The photofragmentation pattern is revealed in the mass spectrum recorded by Fourier Transform of the average of five time-domain transients. The IRMPD spectrum is obtained by plotting the photodissociation yield $R = -\ln(I_{parent}/(I_{parent} + \Sigma I_{fragment}))$ as a function of the wavenumber of the impinging photons. The IR frequency was varied by steps of 2.5 cm^{-1} to span approximately from 600 to 2000 cm^{-1}. To be tunable in this spectral range the electron energy of the FEL was set either at 36 or 48 MeV. The frequency range spanning 450−850 cm^{-1} required the electron energy of the FEL to be set at 30 MeV while flushing the optical table with dry nitrogen to prevent absorption by CO_2. The IR FEL beam is composed of 8 μs long macropulses delivered at 25 Hz. Each macropulse comprises about 500 micropulses, each lasting few picoseconds. A typical average IR power of 0.5 W was obtained, corresponding to a macropulse energy of about 20 mJ.

The kinetics of NO binding to $[Fe^{III}(P)]^+$ ions were recorded on a 4.7T FT-ICR Bruker Spectrospin 47e mass spectrometer upgraded to BioApex with an Apollo I ESI source. The neutral reagent NO was admitted into the cell at a constant pressure in the range of $0.5-12 \times 10^{-8}$ mbar by a leak valve. The pressure readings, obtained from a cold cathode sensor (IKR Pfeiffer Balzers S.p.A., Milan, Italy), were appropriately calibrated.[26] The ESI formed $[Fe^{III}(P)]^+$ ions were allowed to react with NO, and the relative abundances of parent and product ions were analyzed as a function of reaction time to extract kinetic information. The slope of the semilogarithmic plot of the reagent ion abundance versus reaction time yields a pseudo-first order rate constant (k_{obs}) which is divided by the concentration of the neutral reagent to afford the second order rate constant (k_{exp}). The reaction efficiency, $\Phi = k_{exp}/k_{coll} \times 100$, is obtained evaluating k_{coll} using the parametrized trajectory theory.[27]

NO was purchased from Sigma Aldrich, and labeled ^{15}NO was prepared using vacuum line procedures according to the following method. Equimolar amounts (0.028 mol) of $Na^{15}NO_2$ and $FeSO_4$ were placed in a 250 mL three neck round-bottom flask with 28 mL of H_2O at room temperature. Twelve milliliters of a 3 M H_2SO_4 solution were added over a period of 5 min. A deep red vapor immediately developed and dissolved in a few seconds. A stream of helium was constantly maintained through the flask and toward a first trap, kept at −96 °C. A second cooled trap placed in a liquid nitrogen bath was used to condense ^{15}NO coming from the reaction mixture. This second trap was then allowed to warm at room temperature, and ^{15}NO was collected and analyzed by FT-ICR mass spectrometry, showing the product to be 99.9% pure.

Computational Details. The molecular geometries for the $^1A_1$ singlet of $[Fe^{III}(TPP)(NO)]^+$ and of $[Fe^{III}(TPFPP)(NO)]^+$ have been obtained by DFT B3LYP calculations. The standard 6-31G* basis set was used for main group atoms, and consistent 6-31G* type basis set was also used for Fe.[28] The geometry optimization was followed by harmonic frequency calculation both to obtain the theoretical IR spectrum and to ascertain the character of the species, representing a minimum on the potential energy surface. All harmonic frequencies have been corrected by a scaling factor of 0.975 except ν(N−O) which was scaled by a factor of 0.92. To get more insight into the electronic structure associated with the Fe−NO π-bonding interactions, a CASSCF calculation was performed using the B3LYP optimized geometry of the $^1A_1$ state of the $[Fe^{III}(TPP)(NO)]^+$ molecular ion. The active space consisted in 6 electrons distributed in the three nonbonding Fe d and the two NO π^* orbitals. All calculations were performed with the Gaussian03 package program.[29]

■ ASSOCIATED CONTENT

Supporting Information. Figures S1−S5, comparing the IRMPD spectra of the ^{15}N-labeled $[Fe(TPP)(^{15}NO)]^+$ and $[Fe(TPFPP)(^{15}NO)]^+$ complexes with the calculated IR spectra and with the IRMPD spectra of the corresponding unlabeled ions, and complete reference 29. This material is available free of charge via the Internet at http://pubs.acs.org.

■ AUTHOR INFORMATION

Corresponding Author

*E-mail: simonetta.fornarini@uniroma1.it (S.F.), philippe.maitre@u-psud.fr (P.M.).

Present Addresses

[§]School of Chemistry, University of Manchester, Manchester Interdisciplinary Biocenter, 131 Princess Street, Manchester M1 7ND, U.K.

[∥]Department of Chemistry and Biochemistry, University of Bern, Freistrasse 3, CH-3012 Bern, Switzerland.

■ ACKNOWLEDGMENT

This work was supported by the CNRS (PICS program), by the Italian Ministero dell'Istruzione, dell'Università e della Ricerca and by Università di Roma "La Sapienza", and by the European Commission (NEST program, Project No. 15637). The authors are grateful to J. M. Ortega and J. Lemaire and to the technical support at the CLIO facility and to A. Di Marzio for the synthesis of ^{15}NO.

■ REFERENCES

(1) (a) McCleverty, J. A. *Chem. Rev.* **2004**, *104*, 403–418. (b) Murad, F. *Angew. Chem., Int. Ed.* **1999**, *38*, 1856–1868.(c) *Nitric Oxide Chemistry*; Richter-Addo, G. B., Legzdins, P., Burstyn, J., Guest Eds.; *Chem. Rev.* **2002**, *102*, 857.

(2) (a) Cooper, C. E. *Biochim. Biophys. Acta* **1999**, *1411*, 290–309. (b) Bredt, D. S.; Snyder, S. H. *Annu. Rev. Biochem.* **1994**, *63*, 175–195. (c) Butler, A. R.; Williams, D. L. H. *Chem. Soc. Rev.* **1993**, *22*, 233–241. (d) Moncada, S.; Palmer, R. M. J.; Higgs, E. A. *Pharmacol. Rev.* **1991**, *43*, 109–142. (e) Snyder, S. H. *Science* **1992**, *257*, 494–496. (f) Stamler, J. S.; Singel, D. J.; Loscalzo, J. *Science* **1992**, *258*, 1898–1902. (g) Ribeiro, J. M. C.; Hazzard, J. M. H.; Nussenzveig, R. H.; Champagne, D. E.; Walker, F. A. *Science* **1993**, *260*, 539–541.

(3) (a) Macyk, W.; Franke, A.; Stochel, G. *Coord. Chem. Rev.* **2005**, *249*, 2437–2457. (b) Wanat, A.; Wolak, M.; Orzel, L.; Brindell, M.; van Eldik, R.; Stochel, G. *Coord. Chem. Rev.* **2002**, *229*, 37–49. (c) Wyllie, G. R. A.; Scheidt, W. R. *Chem. Rev.* **2002**, *102*, 1067–1090. (d) Scheidt, W. R.; Ellison, M. K. *Acc. Chem. Res.* **1999**, *32*, 350–359. (e) Wolak, M.; van Eldik, R. *Coord. Chem. Rev.* **2002**, *230*, 263–282. (f) Lim, M. D.; Lorkovic, I. M.; Ford, P. C. *J. Inorg. Biochem.* **2005**, *99*, 151–165. (g) Ford, P. C. *Pure Appl. Chem.* **2004**, *76*, 335–350. (h) Ford, P. C.; Lorkovic, I. M. *Chem. Rev.* **2002**, *102*, 993–1017. (i) Cheng, L.; Richter-Addo, G. B. *Porphyrin Handbook* **2000**, *4*, 219–291. (j) Gullotti, M.; Santagostini, L.; Monzani, E.; Casella, L. *Inorg. Chem.* **2007**, *46*, 8971–8975. (k) Ivanovic-Burmazovic, I.; van Eldik, R. *Dalton Trans* **2008**, 5259–5275. (l) Ford, P. C. *Inorg. Chem.* **2010**, *49*, 6226–6239.

(4) Enemark, J. H.; Feltham, R. D. *Coord. Chem. Rev.* **1974**, *13*, 339–406.

(5) (a) Linder, D. P.; Rodgers, K. R.; Banister, J.; Wyllie, G. R. A.; Ellison, M. K.; Scheidt, W. R. *J. Am. Chem. Soc.* **2004**, *126*, 14136–14148.

(b) Tomita, T.; Haruta, N.; Aki, M.; Kitagawa, T.; Ikeda-Saito, M. *J. Am. Chem. Soc.* **2001**, *123*, 2666–2667. (c) Ding, X. D.; Weichsel, A.; Andersen, J. F.; Shokhireva, T. K.; Balfour, C.; Pierik, A. J.; Averill, B. A.; Montfort, W. R.; Walker, F. A. *J. Am. Chem. Soc.* **1999**, *121*, 128–138. (d) Soldatova, A. V.; Ibrahim, M.; Olson, J. S.; Czernuszewicz, R. S.; Spiro, T. G. *J. Am. Chem. Soc.* **2010**, *132*, 4614–4625. (e) Bikiel, D. E.; Bari, S. E.; Doctorovich, F.; Estrin, D. A. *J. Inorg. Biochem.* **2008**, *102*, 70–76. (f) Ellison, M. K.; Schulz, C. E.; Scheidt, W. R. *Inorg. Chem.* **2000**, *39*, 5102–5110.

(6) Thomas, M. R.; Brown, D.; Franzen, S.; Boxer, S. G. *Biochemistry* **2001**, *40*, 15047–15056.

(7) Praneeth, V. K. K.; Paulat, F.; Berto, T. C.; DeBeer George, S.; Näther, C.; Sulok, C. D.; Lehnert, N. *J. Am. Chem. Soc.* **2008**, *130*, 15288–15303.

(8) (a) Richter-Addo, G. B.; Wheeler, R. A.; Hixson, C. A.; Chen, L.; Khan, M. A.; Ellison, M. K.; Schulz, C. E.; Scheidt, W. R. *J. Am. Chem. Soc.* **2001**, *123*, 6314–6326. (b) Roberts, S. A.; Weichsel, A.; Qiu, Y.; Shelnutt, J. A.; Walker, F. A.; Montfort, W. R. *Biochemistry* **2001**, *40*, 11327–11337. (c) Xu, N.; Powell, D. R.; Cheng, L.; Richter-Addo, G. B. *Chem. Commun.* **2006**, 2030–2032. (d) Paulat, F.; Lehnert, N. *Inorg. Chem.* **2007**, *46*, 1547–1549.

(9) Silvernail, N. J.; Barabanschikov, A.; Pavlik, J. W.; Noll, B. C.; Zhao, J.; Alp, E. E.; Sturhahn, W.; Sage, J. T.; Scheidt, W. R. *J. Am. Chem. Soc.* **2007**, *129*, 2200–2201.

(10) (a) Ibrahim, M.; Xu, C.; Spiro, T. G. *J. Am. Chem. Soc.* **2006**, *128*, 16834–16845; (b) Vogel, K. M.; Kozlowski, P. M.; Zgierski, M. Z.; Spiro, T. G. *J. Am. Chem. Soc.* **1999**, *121*, 9915–9921; (c) Spiro, T. G.; Zgierski, M. Z.; Kozlowski, P. M. *Coord. Chem. Rev.* **2001**, *219—221*, 923–936; (d) Lipscomb, L. A.; Lee, B. S.; Yu, N. T. *Inorg. Chem.* **1993**, *32*, 281–286; (e) Wang, Y.; Averill, B. A. *J. Am. Chem. Soc.* **1996**, *118*, 3972–3973; (f) Zeng, W.; Silvernail, N. J.; Wharton, D. C.; Georgiev, G. Y.; Leu, B. M.; Scheidt, W. R.; Zhao, J.; Sturhahn, W.; Alp, E. E.; Sage, J. T. *J. Am. Chem. Soc.* **2005**, *127*, 11200–11201; (g) Praneeth, V. K. K.; Naether, C.; Peters, G.; Lehnert, N. *Inorg. Chem.* **2006**, *45*, 2795–2811; (h) Obayashi, E.; Tsukamoto, K.; Adachi, S.-i.; Takahashi, S.; Nomura, M.; Iizuka, T.; Shoun, H.; Shiro, Y. *J. Am. Chem. Soc.* **1997**, *119*, 7807–7816; (i) Kim, S.; Lim, M. *J. Am. Chem. Soc.* **2005**, *127*, 8908–8909; (j) Derbyshire, E. R.; Gunn, A.; Ibrahim, M.; Spiro, T. G.; Britt, R. D.; Marletta, M. A. *Biochemistry* **2008**, *47*, 3892–3899; (k) Premont-Schwarz, M.; Bohle, D. S.; Gilson, D. F. R. *Inorg. Chim. Acta* **2006**, *359*, 3089–3091; (l) Tomita, T.; Hirota, S.; Ogura, T.; Olson, J. S.; Kitagawa, T. *J. Phys. Chem. B* **1999**, *103*, 7044–7054; (m) Benko, B.; Yu, N.-T. *Proc. Natl. Acad. Sci. U.S.A.* **1983**, *80*, 7042–7046; (n) *Inorg. Chem.* **2010**, *49*, 6223–6774; See also the *Inorganic Chemistry Forum Issue: the Coordination Chemistry of Nitric Oxide and its Significance for Metabolism, Signaling, and Toxicity in Biology.*

(11) (a) MacAleese, L.; Maitre, P. *Mass Spectrom. Rev.* **2007**, *26*, 583–605. (b) Oomens, J.; Van Roij, A. J. A.; Meijer, G.; Von Helden, G. *Astrophys. J.* **2000**, *542*, 404–410. (c) Polfer, N. C.; Oomens, J. *Phys. Chem. Chem. Phys.* **2007**, *9*, 3804–3817. (d) Duncan, M. A. *Int. Rev. Phys. Chem.* **2003**, *22*, 407–435. (e) Dopfer, O.; Solcà, N.; Lemaire, J.; Maître, P.; Crestoni, M. E.; Fornarini, S. *J. Phys. Chem. A* **2005**, *109*, 7881–7887.

(12) (a) Bakker, J. M.; Besson, T.; Lemaire, J.; Scuderi, D.; Maître, P. *J. Phys. Chem. A* **2007**, *111*, 13415–13424. (b) Correia, C. F.; Balaj, P. O.; Scuderi, D.; Maitre, P.; Ohanessian, G. *J. Am. Chem. Soc.* **2008**, *130*, 3359–3370. (c) Chiavarino, B.; Crestoni, M. E.; Fornarini, S.; Lanucara, F.; Lemaire, J.; Maitre, P.; Scuderi, D. *Chem.—Eur. J.* **2009**, *15*, 8185–8195. (d) Bakker, J. M.; Sinha, R. K.; Besson, T.; Brugnara, M.; Tosi, P.; Salpin, J.-Y.; Maitre, P. *J. Phys. Chem. A* **2008**, *112*, 12393–12400. (e) Frison, G.; van der Rest, G.; Tureček, F.; Besson, T.; Lemaire, J.; Maître, P.; Chamot-Rooke, J. *J. Am. Chem. Soc.* **2008**, *130*, 14916–14917.

(13) Crestoni, M. E.; Fornarini, S. *Inorg. Chem.* **2005**, *44*, 5379–5387.

(14) (a) Chen, O.; Groh, S.; Liechty, A.; Ridge, D. P. *J. Am. Chem. Soc.* **1999**, *121*, 11910–11911. (b) Angelelli, F.; Chiavarino, B.; Crestoni, M. E.; Fornarini, S. *J. Am. Soc. Mass Spectrom.* **2005**, *16*, 589–598. (c) Chiavarino, B.; Crestoni, M. E.; Fornarini, S.; Rovira, C. *Inorg. Chem.* **2008**, *47*, 7792–7801.

(15) (a) Ellison, M. K.; Scheidt, W. R. *J. Am. Chem. Soc.* **1999**, *121*, 5210–5219. (b) Jee, J.-E.; van Eldik, R. *Inorg. Chem.* **2006**, *45*, 6523–6534. (c) Hoshino, M.; Maeda, M.; Konishi, R.; Seki, H.; Ford, P. C. *J. Am. Chem. Soc.* **1996**, *118*, 5702–5707.

(16) Chiavarino, B.; Crestoni, M. E.; Fornarini, S.; Lanucara, F.; Lemaire, J.; Maitre, P.; Scuderi, D. *ChemPhysChem* **2008**, *9*, 826–828.

(17) Andrews, L.; Citra, A. *Chem. Rev.* **2002**, *102*, 885–911.

(18) (a) Linder, D. P.; Rodgers, K. R. *Inorg. Chem.* **2005**, *44*, 1367–1380. (b) Linder, D. P.; Rodgers, K. R. *J. Biol. Inorg. Chem.* **2007**, *12*, 721–731.

(19) (a) Wondimagegn, T.; Ghosh, A. *J. Am. Chem. Soc.* **2001**, *123*, 5680–5683. (b) Ghosh, A. *Acc. Chem. Res.* **2005**, *38*, 943–954. (c) Xu, N.; Yi, J.; Richter-Addo, G. B. *Inorg. Chem.* **2010**, *49*, 6253–6266. (d) Nutt, D. R.; Meuwly, M. *ChemPhysChem* **2007**, *8*, 527–536. (e) Lehnert, N.; Sage, J. T.; Silvernail, N.; Scheidt, W. R.; Alp, E. E.; Sturhahn, W.; Zhao, J. *Inorg. Chem.* **2010**, *49*, 7197–7215.

(20) (a) Fomitchev, D. V.; Coppens, P.; Li, T.; Bagley, K. A.; Chen, L.; Richter-Addo, G. B. *Chem. Commun.* **1999**, 2013–2014. (b) Cheng, L.; Novozhilova, I.; Kim, C.; Kovalevsky, A.; Bagley, K. A.; Coppens, P.; Richter-Addo, G. B. *J. Am. Chem. Soc.* **2000**, *122*, 7142–7143. (c) Lee, J.; Kovalevsky, A. Y.; Novozhilova, I.; Bagley, K. A.; Coppens, P.; Richter-Addo, G. B. *J. Am. Chem. Soc.* **2004**, *126*, 7180–7181. (d) Coppens, P.; Novozhilova, I.; Kovalevsky, A. *Chem. Rev.* **2002**, *102*, 861–884.

(21) (a) Olah, J.; Harvey, J. N. *J. Phys. Chem. A* **2009**, *113*, 7338–7345. (b) Radon, M.; Broclawik, E.; Pierloot, K. *J. Phys. Chem. B* **2010**, *114*, 1518–1528. (c) Radoul, M.; Sundararajan, M.; Potapov, A.; Riplinger, C.; Neese, F.; Goldfarb, D. *Phys. Chem. Chem. Phys.* **2010**, *12*, 7276–7289. (d) Scheidt, W. R.; Barabanschikov, A.; Pavlik, J. W.; Silvernail, N. J.; Sage, J. T. *Inorg. Chem.* **2010**, *49*, 6240–6252. (e) Radon, M.; Pierloot, K. *J. Phys. Chem. A* **2008**, *112*, 11824–11832. (f) Blomberg, L. M.; Blomberg, M. R. A.; Siegbahn, P. E. M. *J. Inorg. Biochem.* **2005**, *99*, 949–958. (g) Walker, F. A. *J. Inorg. Biochem.* **2005**, *99*, 216–236. (h) Lehnert, N.; Galinato, M. G. I.; Paulat, F.; Richter-Addo, G. B.; Sturhahn, W.; Xu, N.; Zhao, J. *Inorg. Chem.* **2010**, *49*, 4133–4148. (i) Goodrich, L. E.; Paulat, F.; Praneeth, V. K. K.; Lehnert, N. *Inorg. Chem.* **2010**, *49*, 6293–6316.

(22) Chiavarino, B.; Crestoni, M. E.; Fornarini, S.; Lemaire, J.; Maitre, P.; MacAleese, L. *J. Am. Chem. Soc.* **2006**, *128*, 12553–12561.

(23) Rauhut, G.; Jarzecki, A. A.; Pulay, P. *J. Comput. Chem.* **1997**, *18*, 489–500.

(24) (a) Eyler, J. R. *Mass Spectrom. Rev.* **2009**, *28*, 448–467. (b) Simon, A.; MacAleese, L.; Maitre, P.; Lemaire, J.; McMahon, T. B. *J. Am. Chem. Soc.* **2007**, *129*, 2829–2840.

(25) Paulat, F.; Praneeth, V. K. K.; Naether, C.; Lehnert, N. *Inorg. Chem.* **2006**, *45*, 2835–2856.

(26) Chiavarino, B.; Crestoni, M. E.; Fornarini, S.; Rovira, C. *Chem.—Eur. J.* **2007**, *13*, 776–785.

(27) Su, T.; Chesnavich, W. J. *J. Chem. Phys.* **1982**, *76*, 5183–5185.

(28) Rassolov, V. A.; Pople, J. A.; Ratner, M. A.; Windus, T. L. *J. Chem. Phys.* **1998**, *109*, 1223–1229.

(29) Frisch, M. J. et al. *Gaussian 03*, revision C.02; Gaussian Inc.: Pittsburgh, PA, 2004.